

## Molecular modeling analyses for the effect of alkali metal oxides on graphene

Medhat A. Ibrahim<sup>1,\*</sup>, Hanan Elhaes<sup>2</sup>, Sherif A. El-Khodary<sup>3</sup>, Mohamed Morsy<sup>3</sup>, Ahmed Refaat<sup>1</sup>, Ibrahim S. Yahia<sup>4,5,6</sup>, Heba Y. Zahran<sup>4,5,6</sup>

<sup>1</sup>Spectroscopy Department, National Research Centre, 33 El-Bohouth Str. 12622 Dokki, Giza, Egypt

<sup>2</sup>Physics Department, Faculty of Women for Arts, Science and Education, Ain Shams University, 11757 Cairo, Egypt

<sup>3</sup>Building Physics and Environment Institute, Housing & Building National Research Center (HBRC), Dokki, Giza, Egypt

<sup>4</sup>Research Center for Advanced Materials Science (RCAMS), King Khalid University, Abha 61413, P.O. Box 9004, Saudi Arabia

<sup>5</sup>Advanced Functional Materials & Optoelectronic Laboratory (AFMOL), Department of Physics, Faculty of Science, King Khalid University, P.O. Box 9004, Abhaha, Saudi Arabia

<sup>6</sup>Nanoscience Laboratory for Environmental and Biomedical Applications (NLEBA), Semiconductor Lab., Metallurgical Lab.1., Department of Physics, Faculty of Education, Ain Shams University, Roxy, 11757 Cairo, Egypt

\*corresponding author e-mail address: [medahmed6@yahoo.com](mailto:medahmed6@yahoo.com)

## ABSTRACT

Alkali metal oxides such as CaO, MgO and SrO interacted with graphene. CaO was interacted with graphene through O then through Ca atoms. Graphene is supposed to interact with 1 CaO; 2 CaO; 3 CaO and 4 CaO molecules attached to its corner atoms. Additionally, CaO interacted with graphene through the middle atom of graphene through O of CaO. Each structure is supposed to interact with H<sub>2</sub>S, then two important physical quantities were calculated, namely total dipole moment and HOMO/LUMO band gap energy at B3LYP/3-21g\* level of theory. Results indicated that the total dipole moment of modified graphene is increased while its HOMO/LUMO band gap energy is decreased. This enhances the ability for modified graphene to interact with H<sub>2</sub>S. The lowest bandgap energy (0.1703 eV) was corresponding to 2 MgO/graphene, while the highest total dipole moment (68.6390 Debye) was corresponding to 2 SrO/graphene-H<sub>2</sub>S. Results indicated the suitability of modified graphene to act as a sensor for H<sub>2</sub>S.

**Keywords:** MO; MO/Graphene; Gas sensor; H<sub>2</sub>S; B3LYP/3-21g\*.

## 1. INTRODUCTION

The industrial activities that had grown rapidly have several releases especially for gases which need some kind of control. Therefore, technologies in the field of material science must follow up the increasing demand for modern gas sensors. Different forms of carbon nanomaterials are widely applied as electrochemical sensors [1-4]. Such compounds are efficiently used as sensors for many gases as well as volatile organic compounds [5-6]. Besides electrochemical sensing of reduced graphene oxide, they show also bio-sensing activity [7]. There are many methods widely used for modeling and simulating graphene structures, including density functional theory (DFT) and molecular dynamics (MD) simulations [8-9]. Such theoretical approaches could indicate both structural as well as electronic properties which could explain the application of graphene and develop it as well. Although graphene sheet shows sensitivity as a sensor for some common gaseous molecules, it shows higher sensitivity and reactivity after functionalization of graphene with doping and/or using metal oxides [10]. Although graphene is a member of carbon nanomaterials, it is now the parent of a new family of graphene-based materials [11]. Such a new family is not only for gas sorption but also for energy storage [12]. Increasing the applications of modified graphene comes from the fact that graphene properties are not only a function of its number of layers but also a function of the structural defects [13]. As indicated earlier, such defects could be achieved with doping or decoration, which enhances the ability of graphene to carry out its task.

Moreover, it becomes highly sensitive and selective to act as gas sensor. Continuous work on graphene-based materials indicated its suitability to act as electrochemical biosensors for different materials including ascorbic acid; dopamine; uric acid; amino acid tryptophan as well as detecting nitrite in human serum [14]. Molecular modeling with different levels of theory including both Hartree-Fock and DFT showed potential applications for gas-sensing materials [15-19]. It is utilized to follow up the effect of physical and chemical modifications of PVC to enhance its surface properties and promote it to act as gas sensor [15]. Also, it is utilized to follow up the surface of modified fullerene to detect halides [16] and to study the ability of metal oxide-decorated graphene to act as a sensor for H<sub>2</sub>S [17]. It is also applied to follow up the different electronic properties of edge carboxylated graphene in the form of quantum dots [18-19].

It is indicated earlier that graphene-based metal and metal oxide nanocomposites show a wide range of applications in various fields including electronics, electrochemical and electrical fields [20]. This, in turn, led to a continuous research in the synthesis, characteristics and applications of such class of graphene-based materials. In this work, graphene is modified with three alkali metal oxides CaO, MgO and SrO through graphene corner and middle atoms. The interaction with modified graphene and H<sub>2</sub>S is tried with DFT method at B3LYP/3-21g\* level of theory.

## 2. EXPERIMENTAL SECTION

All the studied structures are subjected to calculations with GAUSSIAN09 softcode [21] at Spectroscopy Department, National Research Centre, Egypt. Graphene was optimized at

DFT:B3LYP [22-24] with 3-21g\* basis set. The total dipole moment (TDM) and HOMO/LUMO band gap energy are calculated at the same level of theory.

## 3. RESULTS SECTION

Before discussing the results, it is important to indicate how model molecules are built. Graphene is indicated in figure 1-a, then graphene is modified as indicated in figures 1 to 5 to form  $N\text{CaO/graphene}$ ;  $\text{NOCa/graphene}$  ( $N=1,2,3,4$ ) before and after interaction with  $\text{H}_2\text{S}$ . Another modification for graphene is tried as indicated in figure 6, in which graphene is modified with three metal oxides to build  $\text{graphene}/2\text{MO.H}_2\text{S}$  ( $\text{MO} = \text{CaO}, \text{MgO}$  and  $\text{SrO}$ ). Accordingly, there are 17 model molecules that could be described as in figures 1 through 6. Figure 1-a, b and c show graphene, graphene modified with CaO and graphene modified with CaO interacted with  $\text{H}_2\text{S}$  respectively. Figure 2-a, b and c present models for graphene modified with 2CaO interacted with  $\text{H}_2\text{S}$ , graphene modified with 3CaO interacted with  $\text{H}_2\text{S}$  and graphene modified with 4CaO interacted with  $\text{H}_2\text{S}$  respectively. Figure 3-a, b and c show models for graphene modified with OCa, graphene modified with OCa interacted with  $\text{H}_2\text{S}$  and graphene modified with 2OCa interacted with  $\text{H}_2\text{S}$  respectively. Figure 4-a, b and c present models for graphene modified with 3OCa interacted with  $\text{H}_2\text{S}$ , graphene modified with 4OCa interacted with  $\text{H}_2\text{S}$  and graphene modified with OCa from the middle carbon atom interacted with  $\text{H}_2\text{S}$  and graphene modified with OCa from the middle carbon atom and 4OCa from edges interacted with  $\text{H}_2\text{S}$  respectively. Finally, figure 6 shows the model for  $\text{graphene}/2\text{MO.H}_2\text{S}$  where the MO is substituted with CaO, MgO and SrO respectively.

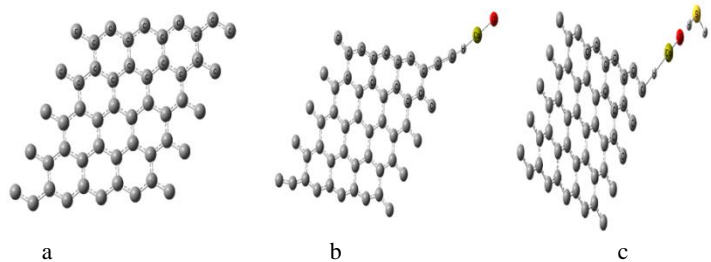


**Figure 1.** B3LYP/3-21g\* model molecules for a-graphene; b-graphene modified with CaO; c-graphene modified with CaO interacted with  $\text{H}_2\text{S}$ .

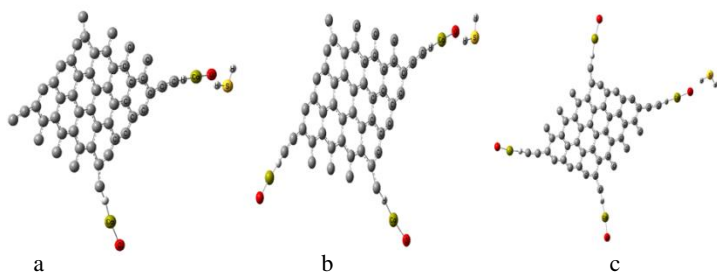


**Figure 2.** B3LYP/3-21g\* model molecules for a- graphene modified with 2CaO interacted with  $\text{H}_2\text{S}$ ; b- graphene modified with 3CaO interacted with  $\text{H}_2\text{S}$ ; c- graphene modified with 4CaO interacted with  $\text{H}_2\text{S}$ .

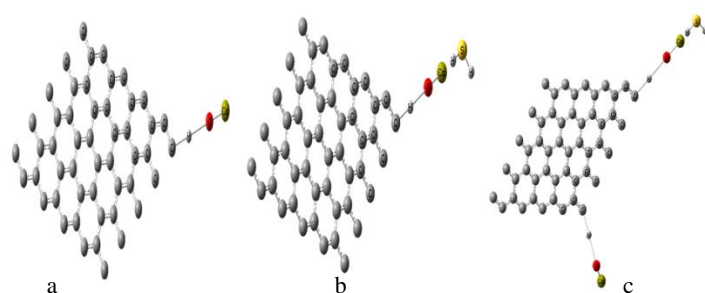


**Figure 3.** B3LYP/3-21g\* model molecules for a- graphene modified with OCa; b- graphene modified with OCa interacted with  $\text{H}_2\text{S}$ ; c- graphene modified with 2OCa interacted with  $\text{H}_2\text{S}$ .

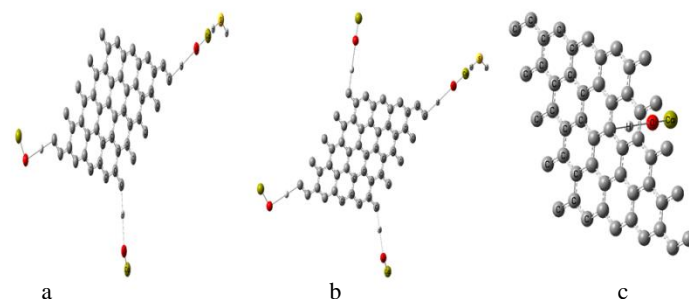


**Figure 4.** B3LYP/3-21g\* model molecules for a- graphene modified with 3OCa interacted with  $\text{H}_2\text{S}$ ; b- graphene modified with 4OCa interacted with  $\text{H}_2\text{S}$ ; c- graphene modified with OCa from the middle carbon atom.

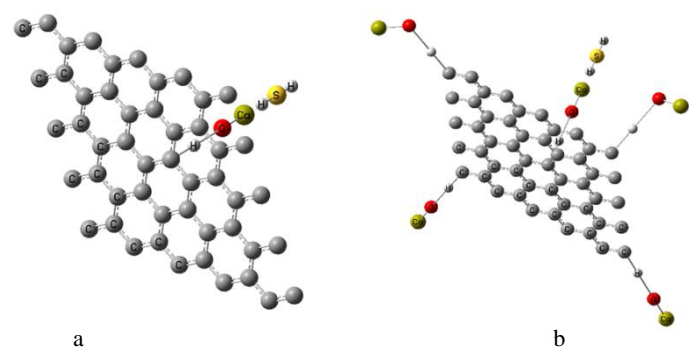


**Figure 5.** B3LYP/3-21g\* model molecules for a- graphene modified with OCa from the middle carbon atom interacted with  $\text{H}_2\text{S}$  and b- graphene modified with OCa from the middle carbon atom and 4OCa from edges interacted with  $\text{H}_2\text{S}$ .

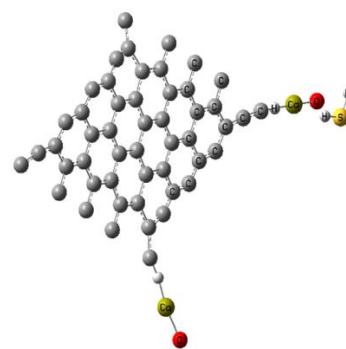


**Figure 6.** B3LYP/3-21g\* model molecules for 2MO/graphene. $\text{H}_2\text{S}$  ( $\text{MO} = \text{CaO}, \text{MgO}$  and  $\text{SrO}$ ).

It is stated earlier in our work that TDM and HOMO/LUMO band gap energy are two important physical quantities related to the reactivity of a given chemical structure [25-26].

The interaction between modified graphene and H<sub>2</sub>S is described with TDM and HOMO/LUMO band gap energy calculated with B3LYP/3-21g\*. Firstly, table 1 presents the TDM for graphene of 0.000 Debye and HOMO/LUMO band gap energy of 0.4740 eV. Then graphene-CaO shows TDM of 28.7180 Debye and band gap energy decreased to 0.1059 eV. After that, CaO/graphene.H<sub>2</sub>S shows the calculated values as 17.7790 Debye and 0.7048 eV. While for 2CaO/graphene.H<sub>2</sub>S, the TDM decreased to be 4.5077 Debye and band gap energy decreased to be 0.1937 eV. As for 3CaO/graphene.H<sub>2</sub>S, the TDM increased to 16.4948 Debye while the band gap energy sharply decreased to be 0.0084 eV. 4CaO/graphene.H<sub>2</sub>S shows also the considerable value of TDM of 8.3325 Debye and the band gap energy of 0.1597 eV. Another interaction between graphene and CaO is tried through O instead of Ca. Table 1 shows also an increase in the TDM to 23.4423 Debye, and band gap energy of 0.4585 eV for OCa/graphene. OCa/graphene.H<sub>2</sub>S shows TDM of 42.7758 Debye and band gap energy of 0.3450 eV. Regarding 2OCa/graphene.H<sub>2</sub>S, the TDM is 43.0800 Debye and band gap energy is 0.5410 eV. The TDM then decreased to be 11.7778 Debye and band gap energy decreased to be 0.4626 eV for graphene/3OCa.H<sub>2</sub>S. 4OCa/graphene. H<sub>2</sub>S shows TDM of 21.7707 Debye and band gap energy of 0.5410 eV. As far as OCa interacted with graphene from the middle (OCa/graphene-middle), the TDM is 14.6786 Debye and band gap energy is 0.2414 eV. OCa/graphene-middle.H<sub>2</sub>S shows calculated values for TDM of 10.3720 Debye and band gap energy of 0.2993 eV. For the last structure 4OCa/graphene-middle.H<sub>2</sub>S, the TDM is 15.3268 Debye and band gap energy is 0.5157 eV. Table 2 presents B3LYP/3-

#### 4. CONCLUSIONS

Graphene has unique surface properties dedicating it for sensing many gases. This computational work indicates that the interaction of graphene with alkali metal oxides enhances its ability for interaction with gases. This kind of metal oxide/graphene composite could act as sensor without further activation of the surface and this enhancement is indicated regardless whether the interaction of metal oxide took place

#### 5. REFERENCES

- [1] Kang I., Heung Y.Y., Kim J.H., Lee J.W., Gollapudi R., Subramaniam S., Narasimhadevara S., Hurd D., Kirikera G.R., Shanov V., Schulz M.J., Shi D., Boerio J., Mall S., Ruggles-Wren M., Introduction to carbon nanotube and nanofiber smart materials, *Compos. B: Eng.*, 37, 382-394, 2006.
- [2] Yun Y.H., Kang I., Gollapudi R., Lee J.W., Hurd D., Shanov V.N., Schulz M.J., Kim J., Shi D., Boerio J.F., Subramaniam S., Multifunctional carbon nanofiber/nanotube smart materials, *Proc. SPIE (Opt. Eng.)*, 5763 184-195, 2005. (Smart Electronics, MEMS, BioMEMS, and Nanotechnology)
- [3] Terrones M., Jorio A., Endo M., Rao A.M., Kim Y.A., Hayashi T., Terrones H., Chaliar J.C., Dresselhaus G., Dresselhaus M.S., New direction in nanotube science, *Mater. Today*, 7, 30-45, 2004.
- [4] Elhaes H., Ibrahim M., Sleim M., Liu J., Huang J., "SnO<sub>2</sub> as a Gas Sensor: Modeling and Spectroscopic approach", *Sens. Lett.*, 7, 530-534, 2009.

21g\* calculated TDM and HOMO/LUMO band gap energy for graphene and 2CaO; 2MgO; 2SrO modified graphene before and after interaction with H<sub>2</sub>S. For 2CaO/graphene.H<sub>2</sub>S, the TDM increased to 4.5077 Debye while the band gap energy is decreased to 0.1937 eV. For graphene/2MgO.H<sub>2</sub>S, the TDM is 4.3909 Debye and band gap energy is 0.1703 eV. Finally, the values of TDM and band gap energy corresponding to graphene-2SrO.H<sub>2</sub>S became 68.6390 Debye and 0.3554 eV respectively.

**Table 1.** B3LYP/3-21g\* calculated TDM as Debye and HOMO/LUMO band gap energy as eV for graphene and CaO modified graphene before and after interaction with H<sub>2</sub>S.

Structure	TDM	ΔE
Graphene	0.0000	0.4740
CaO/Graphene	28.7180	0.1059
CaO/Graphene.H <sub>2</sub> S	17.7790	0.7048
2CaO/Graphene.H <sub>2</sub> S	4.5077	0.1937
3CaO/Graphene.H <sub>2</sub> S	16.4948	0.0084
4CaO/Graphene.H <sub>2</sub> S	8.3325	0.1597
OCa/Graphene	23.4423	0.4585
OCa/Graphene.H <sub>2</sub> S	42.7758	0.3450
2OCa/Graphene.H <sub>2</sub> S	43.0800	0.5410
3OCa/Graphene.H <sub>2</sub> S	11.7778	0.4626
4OCa/Graphene.H <sub>2</sub> S	21.7707	0.5410
OCa/Graphene-Middle	14.6786	0.2414
OCa/Graphene-Middle.H <sub>2</sub> S	10.3720	0.2993
4OCa/Graphene-Middle.H <sub>2</sub> S	15.3268	0.5157

**Table 2.** B3LYP/3-21g\* calculated TDM as Debye and HOMO/LUMO band gap energy as eV for graphene and 2CaO; 2MgO; 2SrO modified graphene before and after interaction with H<sub>2</sub>S.

Structure	TDM	ΔE
Graphene	0.0000	0.4740
2CaO/Graphene.H <sub>2</sub> S	4.5077	0.1937
2MgO/Graphene.H <sub>2</sub> S	4.3909	0.1703
2SrO/Graphene.H <sub>2</sub> S	68.6390	0.3554

through the corner and/or the middle atoms of graphene. Alkali metal oxides increase the TDM and decrease the HOMO/LUMO band gap energy.

In terms of TDM, it is indicated that 2SrO/graphene composite is selective for H<sub>2</sub>S, while from HOMO/LUMO band gap energy perspective; 2MgO/graphene composite is suitable for that task.

- [5] Hsieh C.T., Chen J.M., Kuo R.R., Huang Y.H., Fabrication of well-aligned carbon nanofiber array and its gaseous-phase adsorption, *Appl. Phys. Lett.*, 84, 1186-1188, 2004.
- [6] Roy R.K., Chowdhury M.P., Pal A.K., Room temperature sensor based on carbon nanotubes and nanofibers for methane, *Vacuum*, 77, 223-229, 2005.
- [7] Zhou M., Zhai Y.M., Dong S.J., Electrochemical sensing and biosensing platform based on chemically reduced graphene oxide, *Anal. Chem.*, 81, 5603-5613, 2009.
- [8] Ghaffari R., Alipour K., Solgi S., Irani S., Haddadpour H., Investigation of surface stress effect in 3D complex nano parts using FEM and modified boundary cauchy-born method, *J. Comput. Sci.*, 10, 1-12, 2015.
- [9] Ghaffari R., Duong T.X., Sauer R.A., A new shell formulation for graphene structures based on existing ab-initio data, *Int. J. Solids Struct.*, In Press, 2016.

- [10] Lange U., Hirsch T., Mirsky V.M., Wolfbeis O.S., Hydrogen sensor based on a graphene-palladium nanocomposite, *Electrochim. Acta*, 56, 3707-3712, **2011**.
- [11] Zhang X., Yu L., Wu X., Hu W., Experimental Sensing and Density Functional Theory Study of H<sub>2</sub>S and SOF<sub>2</sub> Adsorption on Au-Modified Graphene, *Adv. Sci.*, 2, 1500101, **2015**.
- [12] Gadipelli S., Guo Z.X., Graphene-based materials: Synthesis and gas sorption, storage and separation, *Prog. Mater. Sci.*, 69, 1-60, **2015**.
- [13] Novoselov K.S., Falco V.I., Colombo L., Gellert P.R., Schwab M.G., Kim K., A roadmap for graphene, *Nature*, 490, 192-200, **2012**.
- [14] Wang X., Gao D., Li M., Li H., Li C., Wu X., Yang B., CVD graphene as an electrochemical sensing platform for simultaneous detection of biomolecules, *Sci. Rep.*, 7, 7044, **2017**.
- [15] Elshaer Y.H., Atta D., El-Mansy M.A.M., Hegazy M.A., Ibrahim M.A., Effect of Solvents and Radiation on the Physical Properties of PVC, *Sensor Lett.*, 16, 311-321, **2018**.
- [16] Ezzat H., Yahia I.S., Zahran H.Y., AlFaify S., Badry R., Elhaes H., Ibrahim M.A., Properties of Fullerene for the Detection of Halides: A Theoretical Approach, *Sensor Lett.*, 16, 217-223, **2018**.
- [17] Hegazy M.A., Elhaes H., El-Khodary S.A., Morsy M., Yahia I.S., Zahran H.Y., AlFaify S., Ibrahim M.A., Molecular Modeling Analyses for ZnO/Graphene as Sensor for H<sub>2</sub>S, *Sensor Lett.*, 16, 17-75, **2018**.
- [18] Abdelsalam H., Elhaes H., Ibrahim M.A., Tuning electronic properties in graphene quantum dots by chemical functionalization: Density functional theory calculations, *Chem. Phys. Lett.*, 138-148, **2018**.
- [19] Abdelsalam H., Elhaes H., Ibrahim M.A., First principles study of edge carboxylated graphene quantum dots, *Physica B*, 537, 77-86, **2018**.
- [20] Khan M., Tahir M.N., Adil S.F., Khan H.U., Siddiqui M.R.H., Alwarthan A.A., Tremel W., Graphene based metal and metal oxide nanocomposites: synthesis, properties and their applications, *J. Mater. Chem. A*, 3, 18753-18808, **2015**.
- [21] Frisch M., Trucks G., Schlegel H., Scuseria G., Robb M., Cheeseman J., Scalmani G., Barone V., Mennucci B., Petersson G., Nakatsuji H., Caricato M., Li X., Hratchian H., Izmaylov A., Bloino J., Zheng G., Sonnenberg J., Hada M., Ehara M., Toyota K., Fukuda R., Hasegawa J., Ishida M., Nakajima T., Honda Y., Kitao O., Nakai H., Vreven T., Montgomery J., Peralta Jr. J., Ogliaro F., Bearpark M., Heyd J., Brothers E., Kudin K., Staroverov V., Keith T., Kobayashi R., Normand J., Raghavachari K., Rendell A., Burant J., Iyengar S., Tomasi J., Cossi M., Rega N., Millam J., Klene M., Knox J., Cross J., Bakken V., Adamo C., Jaramillo J., Gomperts R., Stratmann R., Yazyev O., Austin A., Cammi R., Pomelli C., Ochterski J., Martin R., Morokuma K., Zakrzewski V., Voth G., Salvador P., Dannenberg J., Dapprich S., Daniels A., Farkas O., Foresman J., Ortiz J., Cioslowski J., Fox D., Gaussian 09 Revision C.01, Gaussian Inc., Wallingford CT, **2010**.
- [22] Becke A.D., Density-functional thermochemistry. III. The role of exact exchange, *Chem. Phys.*, 98 5648-5652, **1993**.
- [23] Lee C., Yang W., Parr R.G., Development of the Colle-Salvetti correlation-energy formula into a functional of the electron density, *Phys. Rev. B*, 37, 785-789, **1988**.
- [24] Miehlich B., Savin A., Stoll H., Preuss H., Results obtained with the correlation energy density functionals of Becke and Lee, Yang and Parr, *Chem. Phys. Lett.*, 157, 200-206, **1989**.
- [25] Ibrahim M., El-Haes H., Computational Spectroscopic Study of Copper, Cadmium, Lead and Zinc Interactions in the Environment, *Int. J. Environ. Pollut.*, 23, 417-424, **2005**.
- [26] Ibrahim M., Mahmoud A.A., Computational Notes on the Reactivity of some Functional Groups, *J. Comput. Theor. Nanosci.*, 6, 1523-1526, **2009**.

## 6. ACKNOWLEDGEMENTS

The authors express their appreciation to "The Research Center for Advanced Materials Science (RCAMS)" at King Khalid University for funding this work under grant number RCAMS/KKU/008-18.

© 2018 by the authors. This article is an open access article distributed under the terms and conditions of the Creative Commons Attribution license (<http://creativecommons.org/licenses/by/4.0/>).